

Self-Augmentation: Generalizing Deep Networks to Unseen Classes for Few-Shot Learning

[CS] LCG 8 May 2020
 arXiv:2004.00251v2
 Jin-Woo Seo^{*,1}
 jw.seo@korea.ac.kr
 Hong-Gyu Jung^{*,1}
 hkgjung00@korea.ac.kr
 Seong-Whan Lee²
 sw.lee@korea.ac.kr

¹ Department of Brain and Cognitive Engineering, Korea University, South Korea

² Department of Artificial Intelligence, Korea University, South Korea

Abstract

Few-shot learning aims to classify unseen classes with a few training examples. While recent works have shown that standard mini-batch training with a carefully designed training strategy can improve generalization ability for unseen classes, well-known problems in deep networks such as memorizing training statistics have been less explored for few-shot learning. To tackle this issue, we propose self-augmentation that consolidates self-mix and self-distillation. Specifically, we exploit a regional dropout technique called self-mix, in which a patch of an image is substituted into other values in the same image. Then, we employ a backbone network that has auxiliary branches with its own classifier to enforce knowledge sharing. Lastly, we present a local representation learner to further exploit a few training examples for unseen classes. Experimental results show that the proposed method outperforms the state-of-the-art methods for prevalent few-shot benchmarks and improves the generalization ability.

1 Introduction

Deep networks have achieved remarkable performance in recognition problems [1, 2, 3, 4, 5] over hand-crafted features[6, 7, 8, 9, 10]. Assuming a large-scale training dataset is available, most researchers focus on training deep networks on base classes to test unseen *images* of trained classes. However, there is a growing interest in mimicking human abilities such as generalizing a recognition system to classify *classes* that have never been seen before. In particular, few-shot learning assumes only a few training examples are available for the unseen classes. This is a challenging problem since it is highly possible that a few training examples will lead to network overfitting.

One paradigm for this challenge is meta-learning [8, 11, 12], where a large-scale training set for base classes is divided into several subsets (typically called tasks) and the network learns how to adapt to those tasks. In each task, only a few training examples are given for each class to mimic the environment of a test set for unseen classes.

Meanwhile, recent works have shown that a network trained with standard supervision can produce reasonable performance on unseen classes [10, 11, 12]. In the training phase, this paradigm trains a network using a mini-batch sampled from a large-scale training dataset. In the test phase, unseen classes with a few training examples are evaluated using the same network. Thus, the goal is to develop a framework that is generalizable to unseen classes by fully utilizing the knowledge learned through base classes.

While the latter paradigm is closely related to classifying the unseen images belonging to the base classes, only a few studies have taken advantage of lessons learned from the classical classification problem [10, 11, 12]. To tackle this issue, we take a closer look at the generalization ability of deep networks. It is known that deep networks tend to have almost zero-entropy distributions as the softmax output produces one peaked value for a class [13]. This overconfidence can occur even with randomly labeled training data as deep networks are likely to just memorize the training statistics [14]. In our problem setting, this memorization property directly affects the performance on unseen classes as we rely heavily on the network ability trained on the dataset of base classes. The problem even worsens as we cannot apply a simple transfer learning strategy given that we have only a few training examples for unseen classes. Thus, to overcome the memorization issues, it is important to induce uncertainty in predictions about input images and regularize the posterior probability [8, 15, 16, 17].

To tackle this issue, we propose self-augmentation that incorporates self-mix and self-distillation to improve the generalization ability¹ for few-shot learning. Here, we use the self-augmentation term as we use input and output resources of the network itself to augment the network’s generalization ability. Specifically, as one of regional dropout techniques, we present self-mix, which substitutes a patch of an input image into another patch of the image. With this dropout effect, the generalization ability can be improved as it prevents us from learning specific structures of a dataset. However, we found that an explicit regularization for the posterior probability is necessary to search for a proper manifold for unseen classes. Thus, we utilize a backbone network that has auxiliary branches with its own classifier to enforce knowledge sharing. This sharing of knowledge forces each branch not to be over-confident in its predictions, thus improving the generalization ability. Cooperating with self-mix, experimental results show that self-distillation can significantly boost the performance on unseen classes. Lastly, we propose a local representation learner as a fine-tuning method to exploit a few training examples given for unseen classes. As we train a network on base classes, the goal is to exploit the opportunity to improve the discriminative ability of the network for unseen classes using only 1 or 5 training examples. We will show that this representation learning is especially beneficial to a cross domain problem.

2 Related Work

Few-Shot Learning. The literature on few-shot learning considers training and test datasets that are disjoint in terms of classes. Depending on how the training set is handled, we can categorize it into two main branches: meta-learning and standard supervised learning.

Meta-learning approaches train a network by explicitly emulating the test environment for few-shot learning. Three approaches exist for this paradigm: 1) Metric-learning to reduce the distance among features of different classes [18, 19, 20, 21, 22], 2) optimization-based

¹Henceforth, we denote the term “generalization” as the ability to adapt to unseen classes, given a network trained on base classes.

approaches to initialize a parameter space so that a few training examples of unseen classes can be quickly trained with the cross-entropy loss [8, 13, 17], and 3) weight generation methods to directly generate classification weights used for unseen classes [9, 11, 18].

In contrast, the standard supervised learning trains a network as usual without splitting a training dataset into several tasks. In other words, this approach utilizes the training dataset as in the classical classification problem, but it aims to generalize unseen classes. To achieve this, dense classification applies the classification loss to all spatial information of an activation map to maximally exploit local information [20]. A previous study used self-supervision and showed that the auxiliary loss without labels can extract discriminative features for few-shot learning [10]. An ensemble method using multiple networks was also proposed to resolve the high-variance issue in few-shot learning [1].

Generalization. Many efforts have been made to understand the generalization performance of deep learning [8, 10, 24, 27, 40, 42, 47, 49]. Notably, it has been shown that deep networks easily adapt to random labels and are even well trained for images that appear as nonsense to humans [20]. Along the same lines, many works have found that deep networks produce overconfident classification predictions about an input, thus causing loss in the generalization performance [23, 24, 40, 49]. To resolve this issue, recently, regional dropout [6, 46] and mixing up of two images [11, 48] have been proposed as data augmentation techniques. On the other hands, other researchers showed that label smoothing [39] and knowledge distillation [12, 18, 36, 49] effectively mitigate the overfitting problem by regularizing the posterior probability. In this paper, we expand these findings and indicate that perturbing input and output information should be extensively investigated for few-shot learning. To this end, we propose a training framework that consolidates a novel regional dropout called self-mix and knowledge distillation. In addition, we show that a novel fine-tuning method can be used to boost the performance of few-shot learning.

3 Methodology

3.1 General Framework

In this paper, we are interested in training a network on base classes to be generalizable to unseen classes. Before elaborating on the proposed method, we introduce the general framework for training and inference.

Training. We define a classifier as $C(f(\cdot; \Theta^{1:B}))$, where $f(\cdot; \Theta^{1:B})$ is a feature extractor. Here, we denote the parameters from Block 1 to B as $\Theta^{1:B}$, assuming that we use a block-wise network such as ResNet [13]. For the classifier, we use the cosine similarity that has been exploited for few-shot learning [9, 18]. Thus, the k -th output of the classifier for a training example x_i can be defined as

$$C_k(f(x_i; \Theta^{1:B})) = \text{softmax}(\tau \tilde{f}_i^T \bar{w}_k), \quad (1)$$

where \tilde{f}_i is the L2 normalized feature for x_i and \bar{w}_k is the L2 normalized weight for the k -th class. τ is used as a scale parameter for stabilized training [9, 1]. Based on this definition, C^{Base} is denoted as the classifier using base weights, and similarly C^{Novel} is denoted using novel weights.

Then, we consider the mini-batch training with N_{bs} examples and the cost function for

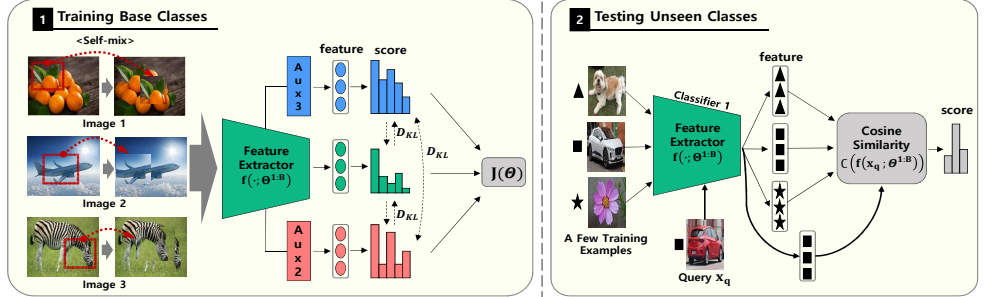


Figure 1: Overview of the proposed self-augmentation framework. The main network consists of three classifiers, two of which are derived from intermediate layers of the main branch. For inference, we use the main classifier to evaluate images from unseen classes.

our training method is expressed as

$$J(\Theta) = \frac{1}{N_{bs}} \sum_{i=1}^{N_{bs}} \ell \left(C \left(f \left(\tilde{x}_i; \Theta^{1:B} \right) \right); \tilde{y}_i \right) + R, \quad (2)$$

where there exist three components: (a) a virtual training example \tilde{x}_i and label \tilde{y}_i , (b) a loss function ℓ and (c) a regularizer R . We sequentially elaborate on the components in the following subsections.

Inference. After training base classes, we consider that a test dataset has C^N classes, which are disjoint to C^B classes for a training dataset. For this measurement, we randomly sample n classes from C^N classes, and pick k examples from each class. The typical numbers for few-shot learning are $n = 5$ and $k = 1$ or 5 . This setting is called n -way k -shot classification. After the sampling process, we generate the weight of the j -th unseen class as follows:

$$w_j^N = \frac{1}{k} \sum_{i=1}^k f_{i,j}, \quad (3)$$

where $f_{i,j}$ is the feature of the i -th example given for the j -th unseen class. Then, a query x_q is classified as

$$\operatorname{argmax}_k C_k^{\text{Novel}} \left(f \left(x_q; \Theta^{1:B} \right) \right), \quad (4)$$

where C_k^{Novel} is defined in Eq. (1) with the above novel weights. We iterate these sampling and inference processes several times to obtain the 95% confidence interval.

3.2 Self-Augmentation

To improve the generalization performance, we propose a training framework called self-augmentation, which consolidates self-mix and self-distillation. The overall architecture of the proposed method is shown in Fig. 1.

3.2.1 Self-Mix

Self-mix is applied to a raw input image to produce a transformed virtual example as follows:

$$\tilde{x} = T(x_i),$$

where $T : x_i[P_1] \rightarrow x_i[P_2]$ denotes by the abuse of notation, the patch P_1 of x_i is replaced by the patch P_2 of x_i . To be specific, we firstly sample a cropping region $P_1 = (r_{a_1}, r_{b_1}, r_w, r_h)$ from an image. The x-y coordinates (r_{a_1}, r_{b_1}) is sampled randomly and (r_w, r_h) is set to a predefined size. If the patch exceeded the image boundary, we crop it. Then, a patch P_2 is sampled with the fixed (r_w, r_h) and (r_{a_2}, r_{b_2}) ($\neq (r_{a_1}, r_{b_1})$) randomly chosen by ensuring not exceeding the image boundary.

Discussion. As regional dropout techniques, there exist two popular works: Cutmix [46] and Cutout [8]. Compared to self-mix, those works have a disadvantage. Cutmix exchanges two randomly selected patches from two images, thus encouraging the network to learn two labels simultaneously. However, it has been reported that such label smoothing impairs the ability of knowledge distillation [23]. Considering that our proposed framework employs knowledge distillation, it is less effective for cutmix to exploit the full capacity of our framework. On the other hands, cutout converts the pixels of the region into zeros, which leads to information loss. To sum up, given that self-mix does not have any information loss and label smoothing issues, we find that it generates a synergy effect with knowledge distillation.

3.2.2 Self-Distillation

Knowledge distillation has been studied to mitigate the overfitting problem by regularizing the posterior probability [14, 18, 56, 49]. Thus, we incorporate self-distillation into our training framework, which employs auxiliary classifiers [18, 56] as shown in Fig. 1. The concept is to create independent predictions for an input image and share the information that has been learned by each classifier. To ensure that the auxiliary classifiers share their own information, we apply the Kullback–Leibler (KL) divergence as a regularizer R [56]. In summary, the general form in Eq. (2) can be modified for our training framework as follows:

$$\begin{aligned} J(\Theta) = & \frac{1}{N_{bs}} \sum_{i=1}^{N_{bs}} \sum_{j=1}^{N_{cls}} \ell \left(C_j^{Base} \left(f \left(\tilde{x}_i; \Theta^{1:l-1} \cup \Theta_j^{l:B} \right) \right); \tilde{y}_i \right) \\ & + \frac{1}{2N_{cls}} \sum_{i=1}^{N_{cls}} \sum_{\substack{j=1, \\ j \neq i}}^{N_{cls}} D_{KL} \left(C_i^{Base} || C_j^{Base} \right). \end{aligned} \quad (5)$$

Here, N_{cls} is the number of classifiers and we use the cross-entropy loss for ℓ . $\Theta^{1:l-1} \cup \Theta_j^{l:B}$ means that the parameters before the l -th block are shared among the classifiers and the $l:B$ blocks are learned independently for the j -th classifier.

3.3 Local Representation Learner

We have proposed how to train a network on base classes to produce global representations, which can be generalizable to unseen classes. In the test stage, we have n -way k -shot training examples and T queries for unseen classes. Thus, we now present how to fine-tune the global representations to yield local representations adjusted for the $n \cdot k$ examples.

Preliminary. For fine-tuning, random transformations are applied on training examples

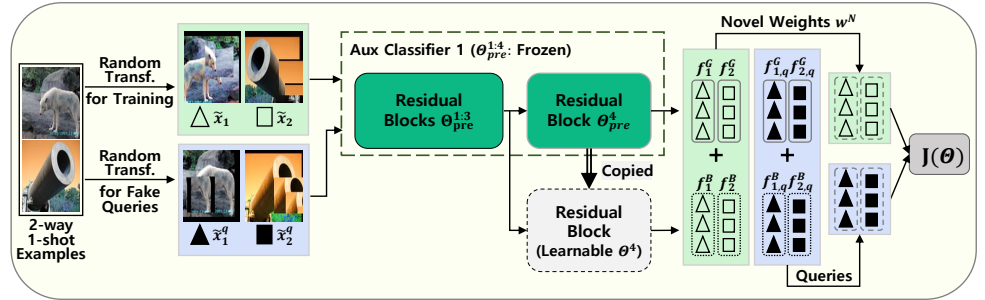


Figure 2: Overview of our local representation learning procedure. We conceptualize our method with an example of 2-way 1-shot learning. We copy the last convolutional block of the network and fine-tune it by exploiting the training examples of unseen classes given for few-shot learning.

to produce novel weights and fake queries as follows:

$$x_1, x_2, \dots, x_{n \cdot k} \xrightarrow[\text{for Training}]{\text{Random Transf.}} \tilde{x}_1, \tilde{x}_2, \dots, \tilde{x}_{n \cdot k}$$

$$x_1, x_2, \dots, x_{n \cdot k} \xrightarrow[\text{for Fake Queries}]{\text{Random Transf.}} \tilde{x}_1^q, \tilde{x}_2^q, \dots, \tilde{x}_{n \cdot k}^q,$$

where \tilde{x}_i is used to create a novel weight and \tilde{x}_i^q is used to induce a loss. For random transformation, we used random color jittering, cropping, horizontal flip and regional dropout such as the proposed self-mix. It is worth noting that we only have access to the $n \cdot k$ examples, and we are never informed about the real queries.

Training. Our objective is not to destroy the well-learned global representations and we promise to be more discriminative after fine-tuning. Thus, we clone the last block of the pre-trained network and only fine-tune the block. The features extracted from the separate networks are denoted as

$$f_i^{Global} := f(\tilde{x}_i; \Theta_{pre}^{1:B})$$

$$f_i^{Bias} := f(\tilde{x}_i; \Theta_{pre}^{1:B-1} \cup \Theta^B),$$

where Θ_{pre} denotes the pre-trained parameters for the base classes. Local representation is defined as the sum of the two features. Similarly, the features for queries can be defined as $f_{i,q}^{Global}$ and $f_{i,q}^{Bias}$. Then, according to Eq. (3), the weight for the j -th unseen class is produced by

$$w_j^N = \frac{1}{k} \sum_{i=1}^k (f_{i,j}^{Global} + f_{i,j}^{Bias}). \quad (6)$$

As we have formed novel weights and features for fake queries, a cost function is defined as

$$J(\Theta) = \frac{1}{n \cdot k} \sum_{i=1}^{n \cdot k} \ell \left(C^{Novel} \left(f_{i,q}^{Global} + f_{i,q}^{Bias} \right); \tilde{y}_i \right) + \gamma \sum_{j=1}^n \sum_{i=1}^k \| f_{i,j}^{Global} - f_{i,j}^{Bias} \|_2, \quad (7)$$

where the regularizer γ prevents the fine-tuned block Θ^B from destroying the well-learned feature space given that only a few training examples are available. Overall, we try to learn the bias term to increase the distance between classes that are close to each other so that they are more distinguishable. The overall concept is illustrated in Fig. 2.

| Method | Backbone | miniImageNet | | tieredImageNet | |
|-------------------------|-----------|-------------------------------------|-------------------------------------|-------------------------------------|-------------------------------------|
| | | 1-shot | 5-shot | 1-shot | 5-shot |
| LEO [19] | WRN-28-10 | 61.76 \pm 0.08% | 77.59 \pm 0.12% | 66.33 \pm 0.05% | 81.44 \pm 0.09% |
| MTL [20] | ResNet12 | 61.20 \pm 1.80% | 75.50 \pm 0.80% | - | - |
| AM3-TADAM [21] | ResNet12 | 65.30 \pm 0.49% | 78.10 \pm 0.36% | 69.08 \pm 0.47% | 82.58 \pm 0.31% |
| MetaOptNet [22] | ResNet12 | 62.64 \pm 0.61% | 78.63 \pm 0.46% | 65.99 \pm 0.72% | 81.56 \pm 0.53% |
| DC [23] | ResNet12 | 62.53 \pm 0.19% | 78.95 \pm 0.19% | - | - |
| CAM [24] | ResNet12 | 63.85 \pm 0.48% | 79.44 \pm 0.33% | 69.89 \pm 0.51% | 84.23 \pm 0.37% |
| CC+Rotation [25] | WRN-28-10 | 62.93 \pm 0.45% | 79.87 \pm 0.33% | 70.53 \pm 0.51% | 84.98 \pm 0.36% |
| CTM [26] | ResNet18 | 64.12 \pm 0.82% | 80.51 \pm 0.13% | 68.41 \pm 0.39% | 84.28 \pm 1.73% |
| Robust 20-dist++ [27] | ResNet18 | 63.73 \pm 0.62% | 81.19 \pm 0.43% | 70.44 \pm 0.32% | 85.43 \pm 0.21% |
| Self-Augmentation | ResNet12 | 65.27 \pm 0.45% | 81.84 \pm 0.32% | 71.26 \pm 0.50% | 85.55 \pm 0.34% |
| Self-Augmentation + LRL | ResNet12 | 65.37 \pm 0.45% | 82.68 \pm 0.30% | 71.31 \pm 0.50% | 86.41 \pm 0.33% |

Table 1: 5-way few-shot classification accuracies on *miniImageNet* and *tieredImageNet* with 95% confidence intervals. All accuracy results are averaged over 2,000 tasks randomly sampled from the test set. LRL denotes the local representation learner.

Inference. A query is classified by the trivial softmax output, but this time we use T real queries. Thus, our proposed local representation learner can be applied to any global representations trained on base classes.

4 Experiments

We evaluate the proposed method on the widely used datasets for few-shot learning. We also perform ablation studies to validate the generalization effects of our methods.

4.1 Experimental Setup

Datasets. *MiniImageNet* [28] consists of 100 classes randomly selected from ILSVRC-2012 [29] and each class has 600 images with 84×84 image size. We follow the split proposed in [29], namely 64, 16 and 20 classes for training, validation and testing, respectively. *TieredImageNet* [30] has 608 classes randomly selected from ILSVRC-2012 [29] and these classes are grouped into 34 higher level categories. They are then split into 20, 6 and 8 categories to further build 351, 91 and 160 classes for training, validation and testing, respectively. A much larger number of images (totally 779, 165 images) are sized by 84×84 .

Evaluation. We report the performance averaged over 2,000 randomly sampled tasks from the test set to obtain the 95% confidence interval. We use $T = 15$ test queries for the 5-way 5-shot and the 5-way 1-shot, as in [29, 31, 32].

Implementation Details. For all the datasets, we report the results using ResNet-12 [19], which has four blocks. Each block consists of three 3×3 Convolution-BatchNorm-LeakyReLU (0.1) and one 2×2 max pooling. The depths of the four blocks are $64 \rightarrow 160 \rightarrow 320 \rightarrow 640$. Auxiliary classifiers are branched from the 2nd and 3rd blocks of ResNet-12. The two auxiliary classifiers have two and one new ResNet blocks, respectively. We use stochastic gradient descent (SGD) with a Nesterov momentum of 0.9 and a weight decay of 0.0005. We fix the scale parameter for the classifier to $\tau = 20$. More detailed contents for our training framework can be found in the supplementary material.

| Method | <i>miniImageNet</i> → CUB | |
|-------------------------|---------------------------|----------------------|
| | 1-shot | 5-shot |
| RelationNet* [18] | 36.86 ± 0.70% | 57.71 ± 0.73% |
| ProtoNet* [19] | 41.36 ± 0.70% | 62.02 ± 0.70% |
| Linear Classifier* [20] | 44.33 ± 0.74% | 65.57 ± 0.70% |
| Cosine Classifier* [21] | 44.51 ± 0.80% | 62.04 ± 0.76% |
| Diverse 20 Full [22] | - | 66.17 ± 0.55% |
| Self-Augmentation | 51.50 ± 0.46% | 72.00 ± 0.39% |
| + LRL | 51.65 ± 0.46% | 74.20 ± 0.37% |

Table 2: 5-way few-shot classification accuracies on the domain shift (*miniImageNet* → CUB) with the 95% confidence intervals. *We re-implemented the official code [20] to evaluate 1-shot accuracies and 5-shot accuracies were reported from [21].

| Method | <i>miniImageNet</i> | | <i>tieredImageNet</i> | | <i>miniImageNet</i> → CUB | |
|--------------------------|----------------------|----------------------|-----------------------|----------------------|---------------------------|----------------------|
| | 1-shot | 5-shot | 1-shot | 5-shot | 1-shot | 5-shot |
| Baseline | 61.42 ± 0.45% | 78.32 ± 0.33% | 68.22 ± 0.50% | 83.21 ± 0.36% | 47.76 ± 0.44% | 67.40 ± 0.38% |
| Cutout | 62.38 ± 0.44% | 79.18 ± 0.33% | 69.40 ± 0.51% | 84.27 ± 0.36% | 47.46 ± 0.44% | 67.79 ± 0.40% |
| Cutmix | 62.81 ± 0.45% | 79.82 ± 0.33% | 69.09 ± 0.49% | 84.21 ± 0.35% | 48.35 ± 0.44% | 67.77 ± 0.39% |
| Selfmix | 62.85 ± 0.45% | 79.83 ± 0.32% | 69.95 ± 0.40% | 84.39 ± 0.35% | 48.73 ± 0.45% | 69.20 ± 0.39% |
| Self-Distillation | 63.11 ± 0.45% | 79.93 ± 0.33% | 70.05 ± 0.49% | 84.92 ± 0.34% | 48.91 ± 0.44% | 69.45 ± 0.38% |
| SD + Cutout | 64.61 ± 0.44% | 81.57 ± 0.31% | 70.76 ± 0.50% | 85.50 ± 0.35% | 48.94 ± 0.43% | 69.65 ± 0.39% |
| SD + Cutout + LRL | 64.93 ± 0.45% | 82.34 ± 0.30% | 70.82 ± 0.50% | 86.15 ± 0.33% | 48.93 ± 0.42% | 73.37 ± 0.36% |
| SD + Cutmix | 64.44 ± 0.45% | 81.58 ± 0.32% | 70.46 ± 0.49% | 85.51 ± 0.34% | 50.43 ± 0.45% | 70.70 ± 0.39% |
| SD + Cutmix + LRL | 64.67 ± 0.45% | 81.52 ± 0.31% | 70.48 ± 0.48% | 85.60 ± 0.34% | 49.88 ± 0.43% | 72.35 ± 0.37% |
| Self-Augmentation | 65.27 ± 0.45% | 81.84 ± 0.32% | 71.26 ± 0.50% | 85.55 ± 0.34% | 51.50 ± 0.46% | 72.00 ± 0.39% |
| SA + LRL | 65.37 ± 0.45% | 82.68 ± 0.30% | 71.31 ± 0.50% | 86.41 ± 0.33% | 51.65 ± 0.46% | 74.20 ± 0.37% |

Table 3: Ablation study on *miniImageNet*, *tieredImageNet* and cross-domain benchmarks. Baseline refers to a vanilla network without any regional dropout techniques. SD and SA denotes self-distillation and self-augmentation, respectively.

4.2 Comparison with the State-of-the-Art Methods

We compare the proposed method with the state-of-the-art algorithms. As shown in Table 1, self-augmentation with the local representation learner (LRL) clearly outperforms the others by a large margin. It is worth noting that recent techniques [20, 19] perform well in certain environments such as 1-shot or 5-shot, or on a certain dataset, while the proposed method works decently in all settings. This indicates that it is worthwhile investigating the generalization ability of the standard supervision in relation to few-shot learning.

4.3 Cross Domain Experiment

After training a network on *miniImageNet*, we perform 5-way classification on CUB [22]. This is a challenging problem as (1) CUB is designed for fine-grained image classification with 200 bird species, (2) the distributions of the these datasets are largely different and (3) we only have 1 or 5 training examples for few-shot learning. With those difficulties, Table 2 shows that self-augmentation significantly surpasses the previous works [19, 20, 18, 23].

4.4 Ablation Study

Regional Dropout. We show that how performance changes by adopting various regional dropout methods and self-distillation. Baseline refers to a network using light augmentation such as random color jittering, cropping and horizontal flipping. Table 3 indicates four

| Method | Baseline | Baseline | | Self-Distillation | | Self-Augmentation | |
|----------------------------|------------|--------------|----------|-------------------|----------|-------------------|----------|
| | | 1-shot | 5-shot | 1-shot | 5-shot | 1-shot | 5-shot |
| Test class | Base class | Unseen class | | | | | |
| w/o label smoothing | 80.22% | 61.42% | 78.32% | 63.11% | 79.93% | 65.27% | 81.84% |
| w label smoothing | 81.36% | 61.27% | 77.03% | 61.96% | 77.45% | 63.29% | 78.24% |
| Gain | (+1.14%) | (-0.15%) | (-1.29%) | (-1.15%) | (-2.48%) | (-1.84%) | (-3.60%) |

Table 4: Effect of label smoothing on miniImageNet. Applying label smoothing to each method decreases their original performances for unseen classes.

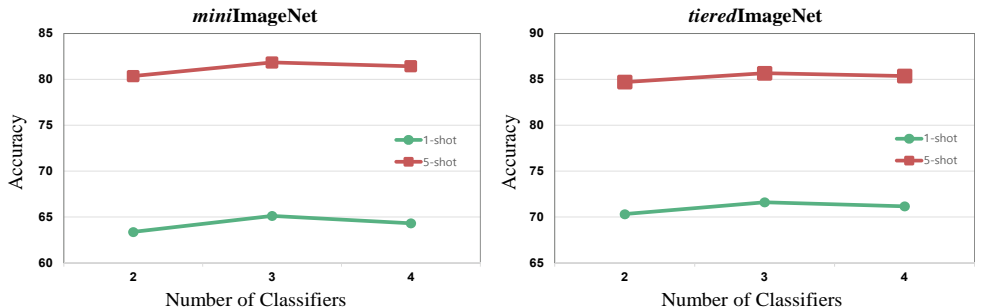


Figure 3: Test accuracies (%) with various numbers of classifiers for self-distillation. In both cases, using three classifiers shows the highest accuracy.

notable aspects: (1) Self-augmentation significantly outperforms the baseline using light augmentation only. (2) Although either regional dropout or self-distillation can improve the generalization capability, exploiting both methods leads to higher performance gains. (3) As discussed in Sect. 3.2.1, the proposed self-mix has a synergistic effect with self-distillation as it does not require pixel removal [8] or mixed labels [46]. (4) When using cutmix [46] for the local representation learner, the performance remains almost the same. As only a few training examples exist, we conjecture that the mixed labels produced by cutmix increase the complexity of fine-tuning. To sum up, although several regional dropout techniques have been studied, self-mix is more flexible to be used with distillation or local representation learning.

Effect of Label Smoothing. As we deal with a memorization problem of deep networks in terms of few-shot learning, we further present the performance with label smoothing, which is another way to perturb output distributions. Though it is well-known that label smoothing is beneficial for standard classification problems [39], Table 4 indicates that label smoothing is not effective for few-shot learning and there exist a significant performance drop with knowledge distillation. It is worth noting that Table 3 shows that cutmix, which learns two labels simultaneously, has less performance gain over self-mix when using self-distillation.

Number of Classifiers. Fig. 3 shows that how different numbers of classifiers for self-distillation affect the classification performance. We can verify that there exists an optimal number of classifiers and this can be seen as the trade-off between the amount of knowledge sharing and the complexity of the parameter space.

5 Conclusion

In this paper, we show that unseen classes with a few training examples can be classified with a standard supervised training. Especially, we aim at generalizing deep networks to unseen classes by alleviating the memorization phenomenon, which is less studied for few-shot learning. To achieve this, we design self-augmentation to perturb the input and output information. We show that the newly proposed regional dropout, called self-mix, produces state-of-the-art results when cooperating with self-distillation. We also present a local representation learner to exploit a few training examples of unseen classes, which improves the performance for all few-shot learning benchmarks and especially works well on a cross-domain task. *More importantly*, we show that existing perturbation methods such as cutmix, cutout and label smoothing are not the optimal choices for few-shot learning as they are not flexible enough to be used with knowledge distillation or local representation learning.

References

- [1] Herbert Bay, Andreas Ess, Tinne Tuytelaars, and Luc Van Gool. Speeded-up robust features (surf). *Computer Vision and Image Understanding*, 110(3):346–359, 2008.
- [2] Luca Bertinetto, Joao F. Henriques, Philip Torr, and Andrea Vedaldi. Meta-learning with differentiable closed-form solvers. In *International Conference on Learning Representations*, 2019.
- [3] Pratik Chaudhari, Anna Choromanska, Stefano Soatto, Yann LeCun, Carlo Baldassi, Christian Borgs, Jennifer Chayes, Levent Sagun, and Riccardo Zecchina. Entropy-sgd: Biasing gradient descent into wide valleys. In *International Conference on Learning Representations*, 2017.
- [4] Wei-Yu Chen, Yen-Cheng Liu, Zsolt Kira, Yu-Chiang Frank Wang, and Jia-Bin Huang. A closer look at few-shot classification. In *International Conference on Learning Representations*, 2019.
- [5] Navneet Dalal and Bill Triggs. Histograms of oriented gradients for human detection. In *Proceedings of the IEEE Conference on Computer Vision and Pattern Recognition*, pages 886–893, 2005.
- [6] Terrance DeVries and Graham W Taylor. Improved regularization of convolutional neural networks with cutout. *arXiv preprint arXiv:1708.04552*, 2017.
- [7] Nikita Dvornik, Cordelia Schmid, and Julien Mairal. Diversity with cooperation: Ensemble methods for few-shot classification. In *Proceedings of the IEEE International Conference on Computer Vision*, pages 3723–3731, 2019.
- [8] Chelsea Finn, Pieter Abbeel, and Sergey Levine. Model-agnostic meta-learning for fast adaptation of deep networks. In *Proceedings of International Conference on Machine Learning*, pages 1126–1135, 2017.
- [9] Spyros Gidaris and Nikos Komodakis. Dynamic few-shot visual learning without forgetting. In *Proceedings of the IEEE Conference on Computer Vision and Pattern Recognition*, pages 4367–4375, 2018.

- [10] Spyros Gidaris and Nikos Komodakis. Generating classification weights with gnn denoising autoencoders for few-shot learning. In *Proceedings of the IEEE Conference on Computer Vision and Pattern Recognition*, pages 21–30, 2019.
- [11] Spyros Gidaris, Andrei Bursuc, Nikos Komodakis, Patrick Pérez, and Matthieu Cord. Boosting few-shot visual learning with self-supervision. In *Proceedings of the IEEE International Conference on Computer Vision*, pages 8059–8068, 2019.
- [12] Chuan Guo, Geoff Pleiss, Yu Sun, and Kilian Q Weinberger. On calibration of modern neural networks. In *Proceedings of International Conference on Machine Learning*, pages 1321–1330, 2017.
- [13] Kaiming He, Xiangyu Zhang, Shaoqing Ren, and Jian Sun. Deep residual learning for image recognition. In *Proceedings of the IEEE Conference on Computer Vision and Pattern Recognition*, pages 770–778, 2016.
- [14] Geoffrey Hinton, Oriol Vinyals, and Jeff Dean. Distilling the knowledge in a neural network. *arXiv preprint arXiv:1503.02531*, 2015.
- [15] Ruibing Hou, Hong Chang, MA Bingpeng, Shiguang Shan, and Xilin Chen. Cross attention network for few-shot classification. In *Advances in Neural Information Processing Systems*, pages 4005–4016, 2019.
- [16] Alex Krizhevsky, Vinod Nair, and Geoffrey Hinton. Cifar-10 and cifar-100 datasets. *URL: <https://www.cs.toronto.edu/kriz/cifar.html>*, 6, 2009.
- [17] Alex Krizhevsky, Ilya Sutskever, and Geoffrey E Hinton. Imagenet classification with deep convolutional neural networks. In *Advances in Neural Information Processing Systems*, pages 1097–1105, 2012.
- [18] Xu Lan, Xiatian Zhu, and Shaogang Gong. Knowledge distillation by on-the-fly native ensemble. In *Advances in Neural Information Processing Systems*, pages 7517–7527, 2018.
- [19] Kwonjoon Lee, Subhransu Maji, Avinash Ravichandran, and Stefano Soatto. Meta-learning with differentiable convex optimization. In *Proceedings of the IEEE Conference on Computer Vision and Pattern Recognition*, pages 10657–10665, 2019.
- [20] Hongyang Li, David Eigen, Samuel Dodge, Matthew Zeiler, and Xiaogang Wang. Finding task-relevant features for few-shot learning by category traversal. In *Proceedings of the IEEE Conference on Computer Vision and Pattern Recognition*, pages 1–10, 2019.
- [21] Yann Lifchitz, Yannis Avrithis, Sylvaine Picard, and Andrei Bursuc. Dense classification and implanting for few-shot learning. In *Proceedings of the IEEE Conference on Computer Vision and Pattern Recognition*, pages 9258–9267, 2019.
- [22] David G Lowe. Distinctive image features from scale-invariant keypoints. *International Journal of Computer Vision*, 60(2):91–110, 2004.
- [23] Rafael Müller, Simon Kornblith, and Geoffrey Hinton. When does label smoothing help? In *Advances in Neural Information Processing Systems*, pages 4694–4703, 2019.

[24] Behnam Neyshabur, Srinadh Bhojanapalli, David McAllester, and Nati Srebro. Exploring generalization in deep learning. In *Advances in Neural Information Processing Systems*, pages 5947–5956, 2017.

[25] Boris Oreshkin, Pau Rodríguez López, and Alexandre Lacoste. Tadam: Task dependent adaptive metric for improved few-shot learning. In *Advances in Neural Information Processing Systems*, pages 721–731, 2018.

[26] Unsang Park, Hyun-Cheol Choi, Anil K Jain, and Seong-Whan Lee. Face tracking and recognition at a distance: A coaxial and concentric ptz camera system. *IEEE Transactions on Information Forensics and Security*, 8(10):1665–1677, 2013.

[27] Gabriel Pereyra, George Tucker, Jan Chorowski, Łukasz Kaiser, and Geoffrey Hinton. Regularizing neural networks by penalizing confident output distributions. *arXiv preprint arXiv:1701.06548*, 2017.

[28] Hang Qi, Matthew Brown, and David G Lowe. Low-shot learning with imprinted weights. In *Proceedings of the IEEE Conference on Computer Vision and Pattern Recognition*, pages 5822–5830, 2018.

[29] Sachin Ravi and Hugo Larochelle. Optimization as a model for few-shot learning. In *International Conference on Learning Representations*, 2017.

[30] Mengye Ren, Eleni Triantafillou, Sachin Ravi, Jake Snell, Kevin Swersky, Joshua B Tenenbaum, Hugo Larochelle, and Richard S Zemel. Meta-learning for semi-supervised few-shot classification. In *International Conference on Learning Representations*, 2018.

[31] Myung-Cheol Roh, Ho-Keun Shin, and Seong-Whan Lee. View-independent human action recognition with volume motion template on single stereo camera. *Pattern Recognition Letters*, 31(7):639–647, 2010.

[32] Olga Russakovsky, Jia Deng, Hao Su, Jonathan Krause, Sanjeev Satheesh, Sean Ma, Zhiheng Huang, Andrej Karpathy, Aditya Khosla, Michael Bernstein, Alexander C. Berg, and Li Fei-Fei. ImageNet Large Scale Visual Recognition Challenge. *International Journal of Computer Vision*, 115(3):211–252, 2015.

[33] Andrei A Rusu, Dushyant Rao, Jakub Sygnowski, Oriol Vinyals, Razvan Pascanu, Simon Osindero, and Raia Hadsell. Meta-learning with latent embedding optimization. In *International Conference on Learning Representations*, 2019.

[34] Karen Simonyan and Andrew Zisserman. Very deep convolutional networks for large-scale image recognition. In *International Conference on Learning Representations*, 2014.

[35] Jake Snell, Kevin Swersky, and Richard Zemel. Prototypical networks for few-shot learning. In *Advances in Neural Information Processing Systems*, pages 4077–4087, 2017.

[36] Dawei Sun, Anbang Yao, Aojun Zhou, and Hao Zhao. Deeply-supervised knowledge synergy. In *Proceedings of the IEEE Conference on Computer Vision and Pattern Recognition*, pages 6997–7006, 2019.

[37] Qianru Sun, Yaoyao Liu, Tat-Seng Chua, and Bernt Schiele. Meta-transfer learning for few-shot learning. In *Proceedings of the IEEE Conference on Computer Vision and Pattern Recognition*, pages 403–412, 2019.

[38] Flood Sung, Yongxin Yang, Li Zhang, Tao Xiang, Philip HS Torr, and Timothy M Hospedales. Learning to compare: Relation network for few-shot learning. In *Proceedings of the IEEE Conference on Computer Vision and Pattern Recognition*, pages 1199–1208, 2018.

[39] Christian Szegedy, Wei Liu, Yangqing Jia, Pierre Sermanet, Scott Reed, Dragomir Anguelov, Dumitru Erhan, Vincent Vanhoucke, and Andrew Rabinovich. Going deeper with convolutions. In *Proceedings of the IEEE Conference on Computer Vision and Pattern Recognition*, pages 1–9, 2015.

[40] Sunil Thulasidasan, Gopinath Chennupati, Jeff Bilmes, Tammooy Bhattacharya, and Sarah Michalak. On mixup training: Improved calibration and predictive uncertainty for deep neural networks. In *Advances in Neural Information Processing Systems*, pages 13888–13899, 2019.

[41] Yuji Tokozume, Yoshitaka Ushiku, and Tatsuya Harada. Between-class learning for image classification. In *Proceedings of the IEEE Conference on Computer Vision and Pattern Recognition*, pages 5486–5494, 2018.

[42] Vikas Verma, Alex Lamb, Christopher Beckham, Amir Najafi, Ioannis Mitliagkas, Aaron Courville, David Lopez-Paz, and Yoshua Bengio. Manifold mixup: Better representations by interpolating hidden states. In *Proceedings of International Conference on Machine Learning*, pages 6438–6447, 2018.

[43] Oriol Vinyals, Charles Blundell, Timothy Lillicrap, Daan Wierstra, et al. Matching networks for one shot learning. In *Advances in Neural Information Processing Systems*, pages 3630–3638, 2016.

[44] Catherine Wah, Steve Branson, Peter Welinder, Pietro Perona, and Serge Belongie. The caltech-ucsd birds-200-2011 dataset. URL: <http://www.vision.caltech.edu/visipedia/CUB-200-2011.html>, 2011.

[45] Chen Xing, Negar Rostamzadeh, Boris Oreshkin, and Pedro OO Pinheiro. Adaptive cross-modal few-shot learning. In *Advances in Neural Information Processing Systems*, pages 4848–4858, 2019.

[46] Sangdoo Yun, Dongyoon Han, Seong Joon Oh, Sanghyuk Chun, Junsuk Choe, and Youngjoon Yoo. Cutmix: Regularization strategy to train strong classifiers with localizable features. In *Proceedings of the IEEE International Conference on Computer Vision*, pages 6023–6032, 2019.

[47] Chiyuan Zhang, Samy Bengio, Moritz Hardt, Benjamin Recht, and Oriol Vinyals. Understanding deep learning requires rethinking generalization. In *International Conference on Learning Representations*, 2017.

[48] Hongyi Zhang, Moustapha Cisse, Yann N Dauphin, and David Lopez-Paz. mixup: Beyond empirical risk minimization. In *International Conference on Learning Representations*, 2018.

- [49] Ying Zhang, Tao Xiang, Timothy M Hospedales, and Huchuan Lu. Deep mutual learning. In *Proceedings of the IEEE Conference on Computer Vision and Pattern Recognition*, pages 4320–4328, 2018.
- [50] Bolei Zhou, Aditya Khosla, Agata Lapedriza, Aude Oliva, and Antonio Torralba. Learning deep features for discriminative localization. In *Proceedings of the IEEE Conference on Computer Vision and Pattern Recognition*, pages 2921–2929, 2016.

Supplementary Material

A Effect of the Local Representation Learner

Fig. 4 shows that there exist cases where the local representation learner (LRL) fixes the deep network to focus on more discriminative parts. As a result, only self-augmentation with LRL correctly classifies the below images. This indicates that a network can be further enhanced even with a few training examples using a carefully designed strategy.

B Evaluation on CIFAR-FS

In this section, we further provide the performance on another few-shot benchmark; CIFAR-FS [2]. This dataset consists of 100 classes randomly selected from CIFAR-100 [10] and each class has 600 images with size 32×32 . The classes are split into 64, 16 and 20 classes for training, validation and testing, respectively. As shown in Table 5, self-augmentation with LRL outperforms other state-of-the-arts methods.

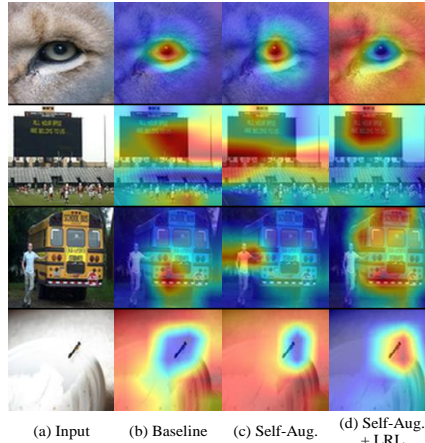


Figure 4: Visualization using the class activation map [50] to show the regions that deep networks focus on.

| Method | Backbone | CIFAR-FS | |
|-------------------------|-----------|--------------------------------------|--------------------------------------|
| | | 1-shot | 5-shot |
| MAML* [8] | C64F | $58.90 \pm 1.9\%$ | $71.50 \pm 1.0\%$ |
| ProtoNet* [25] | C64F | $55.50 \pm 0.7\%$ | $72.00 \pm 0.6\%$ |
| RelationNet* [26] | C64F | $55.00 \pm 1.0\%$ | $69.30 \pm 0.8\%$ |
| R2D2 [1] | C512F | $65.30 \pm 0.2\%$ | $79.40 \pm 0.1\%$ |
| MetaOptNet [10] | ResNet12 | $72.00 \pm 0.7\%$ | $84.20 \pm 0.5\%$ |
| CC+Rotation [2] | WRN-28-10 | $73.62 \pm 0.31\%$ | $86.05 \pm 0.22\%$ |
| Self-Augmentation | ResNet12 | $76.24 \pm 0.47\%$ | $88.39 \pm 0.33\%$ |
| Self-Augmentation + LRL | ResNet12 | $76.25 \pm 0.47\%$ | $88.83 \pm 0.31\%$ |

Table 5: 5-way few-shot classification accuracies on CIFAR-FS with 95% confidence intervals. All accuracy results are averaged over 2,000 tasks randomly sampled from the test set.

*Results from [2].

C Implementation Details

In *miniImageNet*, we trained a network for 60 epochs (each epoch consisted of 1,000 iterations). Initial learning rate was 0.1 and decreased to 0.006, 0.0012 and 0.00024 at 20, 40 and 50 epochs, respectively. In *tieredImageNet*, the network was trained for 100 epochs (each epoch consisted of 2,000 iterations). Initial learning rate was 0.1 and decreased to 0.006, 0.0012 and 0.00024 at 40, 80 and 90 epochs, respectively.

Self-Mix. We randomly sampled a cropping region $P_1 = (r_{x_1}, r_{y_1}, r_w, r_h)$ from an image. Length of the patch (r_w, r_h) was set to $(\frac{W}{2}, \frac{H}{2})$. Then, a patch P_2 from the same input was sampled with randomly chosen $(r_{x_2}, r_{y_2}) \neq (r_{x_1}, r_{y_1})$ and the same (r_w, r_h) . The code-level description is shown in Algorithm 1.

Self-Distillation. We employed three classifiers for self-distillation and two of those were branched from 2nd and 3rd blocks of the backbone. One branch had two blocks and the other branch had one block. All branches were initialized independently, which forces the network into learning different posterior distributions.

Local Representation Learner. For LRL, we used the SGD optimizer and the model was trained for 200 epochs per a task. The initial learning rate was set to the values shown in Table 6 and then decreased by a factor of 10 at 80, 120, 160 epochs. To generate fake queries and novel weights, we applied horizontal flip, random crop, color jittering and then we further applied regional dropout such as self-mix.

Algorithm 1 Pseudo-Code of Self-Mix

```

Input Image with size C× W× H
Length Patch size

1: function SELFMIX(Input, Length)
2:   H = Input.size(2)
3:   W = Input.size(1)
4:   x = randint(0, W)
5:   y = randint(0, H)
6:   x1 = Clip(x - Length/2, 0, W)
7:   x2 = Clip(x + Length/2, 0, W)
8:   y1 = Clip(y - Length/2, 0, H)
9:   y2 = Clip(y + Length/2, 0, H)
10:  while true do
11:    xn = randint(0+(x2 - x1)/2, W-(x2 - x1)/2)
12:    yn = randint(0+(y2 - y1)/2, H-(y2 - y1)/2)
13:    if yn != y or xn != x then
14:      xn1 = xn - (x2 - x1)
15:      xn2 = xn + (x2 - x1)
16:      yn1 = yn - (y2 - y1)
17:      yn2 = yn + (y2 - y1)
18:      break;
19:    end if
20:  end while
21:  Input[:, x1 : x2, y1 : y2] = Input[:, xn1 : xn2, yn1 : yn2]
22: end function

```

| Method | miniImageNet | | tieredImageNet | | miniImageNet \rightarrow CUB | | CIFAR-FS | |
|----------------------|--------------|----------|----------------|----------|--------------------------------|----------|----------|----------|
| | 1-shot | 5-shot | 1-shot | 5-shot | 1-shot | 5-shot | 1-shot | 5-shot |
| LR λ | 1.00E-02 | 1.00E-01 | 1.00E-02 | 1.00E-01 | 1.00E-02 | 1.00E-01 | 1.00E-03 | 1.00E-02 |
| Regularizer γ | 1.00E-01 | 1.00E-01 | 1.00E-01 | 1.00E-01 | 1.00E-01 | 1.00E-01 | 1.00E-02 | 1.00E-02 |

Table 6: Initial learning rates and regularization parameters for the local representation learner.